ADVANCED MATERIALS

diffractometer, 5928 reflections were measured using a graphite-monochromated MoK_α radiation. With 331 variables, the structure was refined using 3100 data points for which $I > 3\sigma(I)$, to a convergence of $R = 0.055$ and $R_w = 0.059$.
[10] D. A. Dixon, J. S. Miller, *J. Am. Chem. Soc.* **1987**, *109*, 3656.
[11] a) As the $[FeC_5Me_5)_2]^{+\oplus}$ (ref. 3a) or $[Bu_4N]^{\oplus}$ salts. b) J. P. Cornelissen, J. H. van Diemen, L. R. Groeneveld, J. P. Haasnoot, A. L. Spek, J. Reedijk, *Inorg. Chem.* **1992**, *31*, 198. c) As the $[FeC_5Me_5)_2]^{+\oplus}$ salt.
[12] J. S. Miller, D. A. Dixon, J. C. Calabrese, C. Vazquez, P. J. Krusic, M. D. Ward, E. Wasserman, R. L. Harlow, *J. Am. Chem. Soc.* **1990**, *112*, 381.
[13] For $g_{Mn} = g_{TCNE} = 2$; $S_{Mn} = 2$, and $S_{TCNE} = 1/2$: a) $\mu_{eff} = \mu_B \{[g^2S(S+1)]_{Mn} + [g^2S(S+1)]_{TCNE}\}^{1/2} = 5.20\ \mu_B$. b) $M_s = \mu_B N[(Sg)_{Mn} + (Sg)_{TCNE}] = 29925$ emuG/mol.
[14] E.g.: M. Verdauger, M. Julve, A. Michalowicz, O. Kahn, *Inorg. Chem.* **1983**, *22*, 2624. M. Drillon, J. C. Gianduzzo, R. Georges, *Phys. Lett. A* **1983**, *96A*, 413. O. Kahn, *Struct. Bond.* **1987**, *68*, 89.
[15] J. Seiden, *Phys. Lett.* **1983**, *44*, L947.
[16] Other magnetic ordering phenomena at both lower and higher temperatures are also being studied.

Preparation of Mixtures of Silicon Oxynitride and Silicon Nitride by the Reaction of Calcium Silicide with Ammonium Chloride

By *Ferdinand Hofer, Walter Veigl,* and *Edwin Hengge**

Silicon nitride materials have great potential for high-temperature, load-bearing applications, such as in heat engines, because of their high strength, high thermal-shock resistance, and good oxidation resistance.[1] On the other hand, silicon oxynitride has also been known as a refractory material for a considerable time.[2] Only a few investigations of this material have been published despite its good oxidation, corrosion and thermal shock resistance.[3–6] However, interest in the use of silicon oxynitride in ceramic composites is increasing.[7] Currently, silicon nitride powders are manufactured mainly by the gas-phase ammonolysis of silicon tetrachloride, and silicon oxynitrides by the reaction of Si_3N_4 with SiO_2.[8] As these methods are troublesome and expensive, alternative methods are of considerable interest.

Such a possibility is given by the long-known reaction of calcium disilicide with ammonium halides which affords a silicon-subnitride with an overall composition $(Si_3N)_n$ and calcium bromide or chloride.[9] Now, we report that this subnitride reacts with nitrogen at 1500 K. This observation makes the long-known reaction of $CaSi_2$ with ammonium halides interesting as a new route to silicon–nitrogen compounds. The structure of the subnitride could not be solved three decades ago due to the lack of reflections in the X-ray diffraction (XRD) patterns. This means that the reaction product is either amorphous or consists of very fine particles. The same situation holds for the pyrolysis product. Nowadays it is possible to characterize such difficult samples by means of analytical electron microscopy (AEM) employing lattice imaging, electron diffraction, energy-dispersive X-ray spectroscopy and electron energy-loss spectroscopy (EELS).

It is the task of this paper to characterize the products of this solid-state reaction by means of AEM and XRD. High purity $CaSi_2$ is the best choice for the test of the reaction, although its practical applications would be limited due to high costs. Therefore, the above-described reaction was performed with technical-grade $CaSi_2$. The disadvantage of solid-state reactions is the presence of impurities (iron, oxygen, elemental silicon) in the reaction products.

Sample type 1 (see Experimental): The XRD-pattern of the silicon subnitride sample (Fig. 1 a) shows only reflections of $CaBr_2$ (or $CaCl_2$), but no silicon phase is detectable which means that the silicon phase is either amorphous or consists of very fine particles (< 50 nm). The electron microscopical

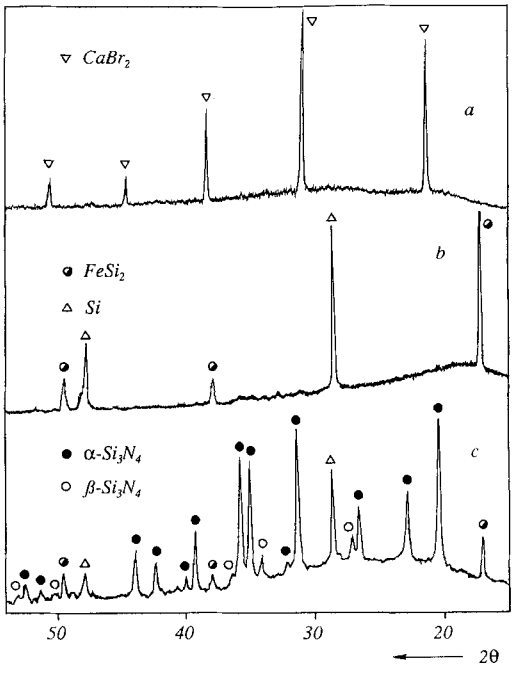

Fig. 1. X-ray diffraction patterns of the reaction products: a) XRD of the product of the reaction of high-purity $CaSi_2$ with ammonium chloride showing reflections of $CaBr_2$. b) XRD of a pyrolysis product (Sample-type 2): technical-grade $CaSi_2$ and ammonium chloride, heated in a quartz reaction tube and washed with water. c) XRD of a pyrolysis product (Sample-type 2): technical-grade $CaSi_2$ and ammonium chloride, heated in a steel tube and washed with water.

investigation of the brown powder showed spongy particles consisting of extremely thin "polymer-like" sheets with a thickness of about 5 to 20 nm. These particles are the major phase of Sample 1 in addition to large $CaCl_2$ or $CaBr_2$ crystals. If technical-grade $CaSi_2$ is used for the reaction, additional minor phases like Si and $FeSi_2$ can be found. Investigations by means of electron diffraction showed that these particles are really amorphous. Elemental analysis of many such particles by EELS showed that the particles consisted of

[*] Dr. F. Hofer [+], W. Veigl, Prof. E. Hengge
Institute of Inorganic Chemistry
Graz University of Technology
Stremayrgasse 16, A-8010 Graz (Austria)
[+] Research Institute for Electron Microscopy

  0935-9648/92/0707-0501 $ 3.50+.25/0

Si, Ca, N and O (Fig. 2a). The analysis of the EEL spectra revealed a remarkable variation of the local chemical compositions: 30–42 at.-% Si, 29–40 at.-% N, 36–13 at.-% O and 5 at.-% Ca. While the Si/N atomic ratio was almost constant, the Si/O atomic ratio varied much more. The near-edge fine structure of the L_{23} edge of silicon (Fig. 2a) clearly shows that the silicon is mainly bound to nitrogen. The ionization threshold lies at 103 eV ($\pm$0.5 eV) thus revealing a chemical shift that is typical for silicon nitrides.[10]. If the brown powder is kept some days under an inert atmosphere EELS analyses showed that the oxygen content is increased in relation to nitrogen. The fine structure of the L_{23} edge of silicon changed to one that looks more similar to Si–O compounds than to Si–N compounds. All this indicates that the Si–N bonds of the silicon nitride are extremely reactive, an observation which has not been previously reported.[9] Therefore, we could not identify a silicon subnitride by AEM immediately, but we found an amorphous polymer-like compound consisting mainly of Si, N and O. Furthermore, it is clear that Si–N bonds are created by this reaction.

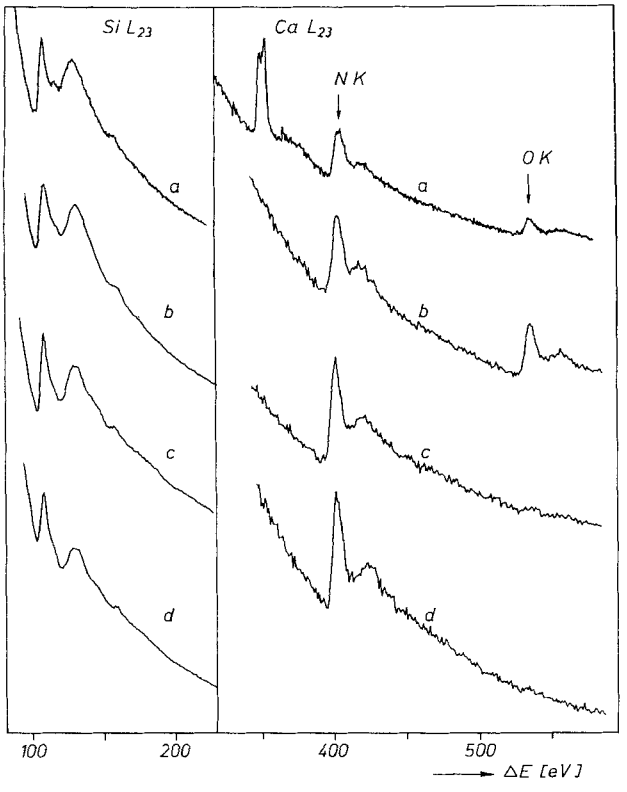

Fig. 2. EEL spectra of the reaction products: a) Amorphous silicon oxynitride in Sample-type 1. b) Silicon oxynitride particle from Sample-type 2 (see also Fig. 3). c) Silicon oxynitride particle from Sample-type 2 after electron irradiation in the TEM. d) Si_3N_4 fiber from Sample-type 2 (see also Fig. 5).

Sample type 2 (see Experimental): To investigate the use of the above described silicon compound as a starting material for the synthesis of Si_3N_4, we heated Sample type 1 materials under nitrogen. Subsequently, the soluble parts of the sample were completely removed by washing with dilute HCl.

The XRD patterns of the washed reaction products clearly depend on the reaction conditions (Fig. 1b and 1c). If a reaction chamber consisting of quartz is used for the pyrolysis no reflections of silicon nitride could be found besides the reflections caused by the minor impurities like Si and $FeSi_2$ (Fig. 1b). However, if a carbon or steel tube is used as reaction chamber, α-Si_3N_4 and β-Si_3N_4 are found besides the impurities (Fig. 1c).

The AEM investigation showed the Sample-type 2 materials to consist mainly the plate-like particles and varying amounts of fibers:

Plate-like particles: Figure 3 shows a typical plate-like particle that consists of very thin sheets (thickness around 10 nm) which are oriented parallel to the direction of the electron beam. The investigation of single sheets of such a

Fig. 3. TEM image of a silicon oxynitride particle consisting of thin plates oriented parallel to the viewing direction (Sample-type 2); the corresponding EEL spectrum is shown in Fig. 2b.

particle showed that they consist of extremely small grains with an average size of 4 nm (Fig. 4). The electron diffractions of these particles gave reflections which could be assigned to Si_2N_2O[11] and and sometimes reflections due to α-Si_3N_4 have been found.

Fig. 4. TEM image of a single silicon oxynitride plate oriented perpendicular to the viewing direction (Sample-type 2) showing the fine particles.

0935-9648/92/0707-0502 $ 3.50+.25/0

ADVANCED MATERIALS

The analysis of these particles by EELS (Fig. 2b) confirmed the occurrence of Si, N and O. The quantification of many such spectra gave compositions almost identical to Si_2N_2O. The N/O ratio can vary slightly in different specimen regions caused by varying amounts of α-Si_3N_4 within the plate-like particles.

Through high-intensity electron irradiation (focused beam and condensor aperture removed) the Si_2N_2O particles decomposed into Si_3N_4, the EEL-spectrum of which is shown in Figure 2c. This reaction occurred via the loss of SiO which condensed near the decomposed particle and which could be analyzed by EELS. However, this decomposition is different from that found by Das Chowdhury et al.,[12] where electron irradiation of Si_2N_2O mainly lead to the loss of nitrogen.

Fibers: Besides the Si_2N_2O particles we found varying amounts of fibers. The TEM image (Fig. 5) shows such a fiber. Electron diffraction showed the material to consist of α-Si_3N_4. Additionally, this result could be confirmed by many EELS analyses of different fibers which gave a Si/N ratio almost identical to Si_3N_4 with only a low oxygen impurity level (Fig. 2d).

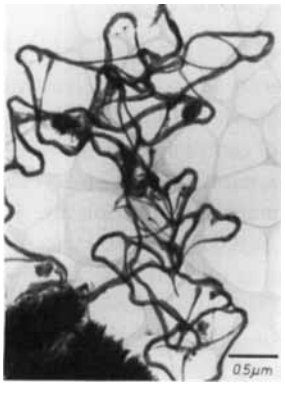

Fig. 5. TEM image of a typical Si_3N_4 fiber (Sample-type 2); the corresponding EEL spectrum is shown in Fig. 2d.

These two phases could be found in all samples, although the Si_3N_4 content varies according to the reaction conditions. If the sample is prepared in a quartz reaction chamber, mainly Si_2N_2O particles can be found and only a few fibers ($\sim$15 wt.-% Si_3N_4). Due to the small particle size of these compounds they are undetectable with XRD (Fig. 1b). As it is indicated by the XRD pattern (Fig. 1c) a reaction performed in a carbon or steel tube leads to an increase of Si_3N_4 fibers and again to Si_2N_2O particles which are also undetectable using XRD ($\sim$30 wt.-% Si_3N_4). Thus, the reaction of calcium silicide and ammonium chloride provides a new route to silicon nitride and silicon oxynitride powders. The reaction products are interesting due to their small particle size and because the Si_3N_4/Si_2N_2O ratio can be varied through adjusting the reaction conditions. However, it was not possible until now to prepare pure silicon nitride with this method and due to the use of technical-grade $CaSi_2$, impurities like Si, $FeSi_2$ and SiO_2 are unavoidable. Additionally, it has to be stated that Si_3N_4 and Si_2N_2O are exclusively formed if high-purity $CaSi_2$ is used and, furthermore, the impurities can be avoided. However, high-purity $CaSi_2$ is too expensive for technical applications.

Several conclusions can be drawn:

- The reaction of $CaSi_2$ with NH_4Cl gave a mixture of $CaCl_2$ and of a silicon-nitride phase. The presence of Si–N bonds in the reaction product could be confirmed by EELS although it was not possible to identify the silicon subnitride directly by AEM due to the extremely high reactivity of the compound.
- The pyrolysis products consisted mainly of Si_2N_2O with a very small grain size (several nm) and varying amounts of α-Si_3N_4 fibers (5 to 30%). The fraction of α-Si_3N_4 could be increased through the careful exclusion of water and oxygen.
- We have found that it is possible to decompose the Si_2N_2O particles into Si_3N_4 by electron irradiation directly in the electron microscope.
- One interesting feature of the silicon oxynitride formed is the extremely small particle size (3–10 nm) which may make this compound interesting in technical applications.

Experimental

The starting material used in this study was technical-grade calcium silicide of the following composition: 33.5 wt.-% Ca, 46.4 wt.-% Si, 7.2 wt.-% $FeSi_2$, 9.0 wt.-% Si (free) and 3.9 wt.-% oxide residue. The $CaSi_2$ powder was milled immediately before the reaction under nitrogen, and mixed with NH_4Cl or NH_4Br and subsequently heated at 620 K under nitrogen. The reaction proceeded very rapidly and resulted in a brown powder which is very sensitive to moisture and oxygen. By-products are calcium halide, hydrogen and ammonia (Sample type 1): $3\,CaSi_2 + 6\,NH_4Cl(Br) \rightarrow 3\,Si_3N + 3\,CaCl_2 + 4\,NH_3 + 6\,H_2$.

In a second step the silicon subnitride was heated to 1500 K under an atmosphere of nitrogen (in a quartz tube) for a period of 5 hours and subsequently washed with dilute HCl to avoid basic conditions and to remove soluble components such as $CaCl_2$ (or $CaBr_2$). The resulting brown powder is stable in air (Sample type 2).

Chemical analysis: The chemical analysis of Sample type 1 yields 20.6 wt.-% Ca, 24.1 wt.-% Si (excluding elemental silicon), 42.55 wt.-% Cl, 5.36 wt.-% N and 7.4 wt.-% impurities (mainly iron and elemental silicon). This led to a molar ratio of 1:2 for Ca and Cl and of 1:0.38 for Si and N, thus confirming the results of the previous investigation. [9] The chemical analysis of the Sample type 2 does not show any calcium and chlorine content. In view of the general composition, the fraction of impurities is higher, about 15%. The content of silicon (excluding elemental silicon) is about 35 wt.-% and nitrogen 18 wt.-%. The difference to 100% seems to be oxygen, about 30 wt.-%. The increased amount of oxygen can easily be explained because during the washing process with water, some silicon nitride and probably some Si–Cl bonds are hydrolyzed. The general composition of the compound is $Si_2O_3N_2$, although the oxygen content varies somewhat in different samples. Before the washing operation, the composition is $Si_3O_2N_2$ (excluding $CaCl_2$ and impurities). In the electron microscopical investigation one can see that this overall compositions represents mixtures of silicon nitride and silicon oxynitrides.

Electron microscopical investigations: The samples were investigated in a Philips EM420 transmission electron microscope (TEM) which was equipped with an energy-dispersive X-ray detector and an electron energy-loss spectrometer (Gatan 607). The microscope was operated at 120 kV. The samples were dispersed on holey carbon foils immediately after the reaction and rapidly placed into the microscope. The oxidation-sensitive Sample 1 was handled under a stream of high-purity nitrogen. The local composition of the samples was derived from the EEL-spectra by procedures which have been described previously. [13] The quantification of these spectra was done by means of experimentally determined scattering cross-section ratios (EELS k-factors). [14] The

  0935-9648/92/0707-0503 $ 3.50+.25/0

X-ray diffraction data were recorded with a Siemens one-circle diffractometer employing Cu-Kα radiation.

Received: January 2, 1992
Final version: May 18, 1992

[1] G. Ziegler, J. Heinrich, G. Wötting, *J. Mater. Sci.* **1987**, *22*, 3041.
[2] M. E. Washburn, *Am. Ceram. Soc. Bull.* **1967**, *46*, 667.
[3] P. Bloch, J. C. Glandus, *J. Mater. Sci.* **1979**, *14*, 379.
[4] J. C. Glandus, P. Bloch, *Energy Ceram.* **1980**, 661.
[5] M. B. Trigg, K. H. Jack, in *Proc. Int. Symp. Ceramic Components for Engines*, Japan, **1983**, (Eds.: S. Somiya, E. Kanai, K. Ando) KTK Scientific Publishers, Tokyo, Japan, **1984**, pp. 199–207.
[6] S. A. Siddiqi, A. Hendry, *Br. Ceram. Proc.* **1986**, *37*, 1.
[7] S. Iio, H. Yokoi, M. Watanabe, Y. Matsuo, *J. Am. Ceram. Soc.* **1991**, *74*, 296.
[8] Z. K. Huang, P. Greil, G. Petzow, *Ceram. Int.* **1984**, *10*, 14.
[9] E. Hengge, *Z. Anorgan. Allg. Chem.* **1962**, *315*, 298.
[10] W. M. Skiff, R. W. Carpenter, S. H. Lin, *J. Appl. Phys.* **1985**, *58*, 3463.
[11] I. Idrestedt, C. Brosset, *Acta Chem. Scand.* **1964**, *18*, 1879.
[12] K. Das Chowdhury, R. W. Carpenter, J. K. Weiss, in *Proc. 47 Annu. Mtg. Electron Microsc. Soc. America* (Ed.: G. W. Bailey) San Francisco Press, San Francisco **1989**, pp. 428–429.
[13] R. F. Egerton. *Electron Energy-Loss Spectroscopy in the Electron Microscope*, Plenum Press, London, **1986**.
[14] F. Hofer, *Microsc. Microanal. Microstruct.* **1991**, *2*, 215.

Magnetic Ordering in a Molecular Material Containing Dysprosium(III) and a Nitronyl Nitroxide**

By *Cristiano Benelli, Andrea Caneschi, Dante Gatteschi,** and *Roberta Sessoli*

Molecular-based magnetic materials are the focus of active research[1] because it is felt that they can provide new types of magnetic behavior associated with the physical and chemical properties which are typical of molecular compounds.

Several systems have already been reported,[2] which order as both bulk ferro- und ferrimagnets. Several approaches are followed in order to increase the critical temperatures. We want to show here how the anisotropy of the magnetic interaction between the interacting centers can drastically increase the transition temperature to magnetic order, and how molecular materials containing rare earths can have magnetic transition temperatures comparable to those of materials containing transition-metal ions.

$M(hfac)_3NITR$ (hfac = hexafluoroacetylacetonate, NITR = 2-*R*-4,4,5,5-tetramethyl-4,5-dihydro-1-*H*-imidazolyl-1-oxyl-3-oxide, M = Y, Gd, Dy) have been found to possess a one-dimensional structure which affects their magnetic properties.[3,4] When M = Y the material behaves as a one-dimensional antiferromagnet,[3] and no evidence of long-range magnetic order is observed above 4.2 K. When M = Gd the behavior is more complex, corresponding to a one-dimensional antiferromagnet dominated by next-nearest-neighbor exchange interactions.[4] However, the material does not show long-range order down to 1.4 K, indicating weak inter-chain interactions, in agreement also with EPR data.

We have now synthesized $Dy(hfac)_3(NITEt)$ and found it isomorphous with the Y analogue.[5] The X-ray determination showed that $Dy(hfac)_3(NITEt)$ has a chain-like structure, with the $Dy(hfac)_3$ moieties bridged by the NITEt radicals (Fig. 1). As in the other rare-earth derivatives the chains

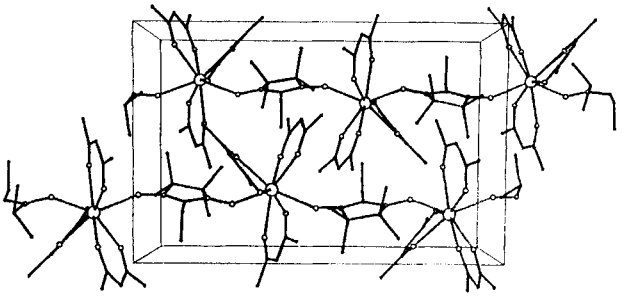

Fig. 1. Unit cell representation for $Dy(hfac)_3(NITEt)$.

are well separated from each other: in the NITEt derivative the shortest interchain Dy–Dy distance is 10.95 Å, which is the shortest observed in this type of compounds, while within the chain the Dy atoms are separated by 8.74 Å. The temperature dependence of the magnetic susceptibility, χ, has been measured both with a SQUID susceptometer in various magnetic fields and with an ac susceptometer operating at different frequencies.

The room-temperature value of χT (12.1 emu mol^{-1}K) measured in a field of 0.5 T is close to the value expected for non-interacting radical and dysprosium(III) ion. The susceptibility follows a Curie–Weiss law down to ca. 30 K, with $\theta = -6.2$ K. The dc susceptibility goes through a narrow

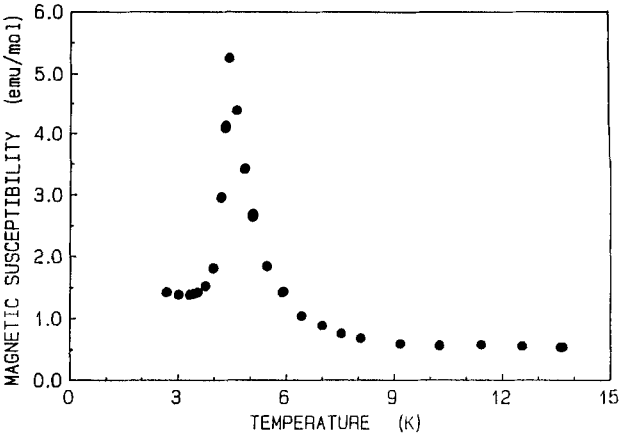

Fig. 2. Temperature dependence of the magnetic susceptibility (emu mol^{-1}) for $Dy(hfac)_3(NITEt)$ in a field of 5 mT.

[*] Prof. Dr. Gatteschi, Dr. C. Benelli, Dr. A. Caneschi, Dr. R. Sessoli
Department of Chemistry, University of Florence
Via Maragliano 75/77, I-50144 Florence (Italy)

[**] The financial support of Progetto Finalizzato materiali Speciali per Tecnologie Avanzate, CNR is gratefully acknowledged.

0935-9648/92/0707-0504 $ 3.50+.25/0